ELSEVIER

Journal of Hazardous Materials B136 (2006) 706–713

Journal of Hazardous Materials

www.elsevier.com/locate/jhazmat

# Effects of ferrous ions on the reductive dechlorination of trichloroethylene by zero-valent iron

Chih-Chung Liu, Dyi-Hwa Tseng *, Chun-Yuan Wang

*Graduate Institute of Environmental Engineering, National Central University, Chungli, Taiwan 32001, ROC*

Received 8 April 2005; received in revised form 29 December 2005; accepted 30 December 2005
Available online 28 February 2006

**Abstract**

The surface characteristics of zero-valent iron (ZVI) and the efficiency of reductive dechlorination of trichloroethylene (TCE) in the presence of ferrous ions were studied. The experimental results indicated that the acid-washing of a metallic iron sample enhanced the efficiency of TCE degradation by ZVI. This occurred because acid-washing changed the conformation of oxides on the surface of iron from maghemite ($\gamma$-$Fe_2O_3$) to the more hydrated goethite ($\alpha$-FeOOH), as was confirmed by XPS analysis. However, when ferrous ions were simultaneous with TCE in water, the TCE degradation rate decreased as the concentration of ferrous ion increased. This was due to the formation of passive precipitates of ferrous hydroxide, including maghemite and magnetite ($Fe_3O_4$), that coated on the surface of acid-washed ZVI, which as a result inhibited the electron transfer and catalytic hydrogenation mechanisms. On the other hand, in an $Fe^0$-TCE system without the acid-washing pretreatment of ZVI, ferrous ions were adsorbed into the maghemite lattice which was then converted to semiconductive magnetite. Thus, the electrons were transferred from the iron surface and passed through the precipitates, allowing for the reductive dechlorination of TCE.


*Keywords:* Zero-valent iron; Iron oxides; Ferrous; Trichloroethylene; Reductive dechlorination

## 1. Introduction

During the past decade, permeable reactive barriers (PRBs) have received a great deal of attention as an innovative, cost-effective technology for the in situ remediation of groundwater contaminated with chlorinated solvents [1–3]. Although a variety of materials have been proposed for use in PRBs, zero-valent iron (ZVI) has shown the greatest promise, especially for the reduction of many common environmental contaminants [4,5]. However, due to the thermodynamic instability of ZVI in the presence of the water, changes in environmental conditions encourage the development of a surface layer of corrosion.

It follows that understanding the behavior of such a layer upon contact with the solution to which it is exposed is important, because of chemical deposit that occurs due to iron corrosion can inhibit electron transfer and catalytic hydrogenation between any contaminants and the iron. Several studies have shown that passive films, formed by mineral precipitation on an iron surface, can cause a rapid decrease of degradation of chlorinated hydrocarbons, by inhibiting access to the reactive iron surface [6,7]. In addition, one can expect porosity loss and reduced flow in the bulk iron material, meaning that the longevity of favorable barrier hydraulics and reactivity must be compensated for [8,9].

Numerous investigations have demonstrated that various kinds of passive films can be coated on iron. Each has a different structure and composition, which depends upon their formation mechanism [10]. In the case of a fresh cathodically cleaned Fe surface, a quasi-bulk $Fe(OH)_2/Fe_3O_4$ film should be expected. An $Fe^{3+}$ film should form on a pre-oxidized Fe surface, which will then be reduced to form a $Fe_3O_4/Fe(OH)_2{\cdot}2FeOOH$ film [11]. In both cases, the main surface product of the aged film is magnetite ($Fe_3O_4$). Magnetite, being a denser species, should occupy the inner layer of the film. Magnetite can also be electrically conductive, which allows a charge to be transferred through the interphase, which in turn induces reductive dechlorination. However, the degradation is slower, since the charge transfer rate through an oxide is slower than on a bare metal surface [12]. Bonin et al. [13] identified magnetite, hydrated magnetite [$Fe(OH)_2{\cdot}2FeOOH$] and green rust complexes as being the final

* Corresponding author. Tel.: +886 3 4226944; fax: +886 3 4226944.
*E-mail address:* dhtseng@ncuen.ncu.edu.tw (D.-H. Tseng).

0304-3894/$ – see front matter © 2006 Elsevier B.V. All rights reserved.
doi:10.1016/j.jhazmat.2005.12.045

products of surface redox reactions that occurred in a borate buffer solution after iron was exposed to the contaminant. Aging the film converted the hydrated magnetite to magnetite. Magnetite and green rust are not protective, so that charge transfer and reductive dechlorination continued.

In addition, in natural subsurface environments, high concentrations of dissolved $Fe^{2+}$, related to the reductive dissolution of ferric oxides and oxyhydroxides, are primarily generated by chemical, physical or biological processes. Moreover, in PRB systems, dissolved $Fe^{2+}$ can also be generated and released into the subsurface environment due to the oxidation of metallic iron. Johnson et al. [14] showed that dehalogenation by surface-bond $Fe^{2+}$ appears to happen faster when there is an oxide film on ZVI. $Fe^{2+}$ reacts with the oxide surface, and electrons are transfer between the adsorbed $Fe^{2+}$ and the underlying $Fe^{3+}$ oxide. This electron transfer induces the growth of an $Fe^{3+}$ layer on the oxide surface that is similar to the bulk oxide [15]. The resulting oxide is capable of reducing chlorinated aliphatics, nitrate, nitroaromatics and uranium [16–20]. The degradation rate and efficiency is dependent on the environmental conditions, such as the pH value, concentration of $Fe^{2+}$, the morphologies of the minerals, and the presence of transitional metal ions.

However, the results from the literatures cited above reveal that little attention has thus far been paid to the production and role of $Fe^{2+}$, and, in particular, its interaction with the corrosion products. Consequently, the objective of this study is to understand how ferrous ions may affect the reductive dechlorination of trichloroethylene (TCE) by ZVI and to clarify the relationship between the ZVI and the passive precipitates of iron (hydro) oxides that coat the iron surface, in the presence of ferrous ions.

## 2. Experimental

### 2.1. Chemicals and materials

The laboratory grade iron, purchased from the Riedel-deHaën Company, had the following characteristics: (1) a particle size of between 0.045 and 0.125 mm; (2) a specific surface area of 0.287 $m^2/g$ (as determined by ASAP 2010 micromeritics using nitrogen BET analysis); (3) a purity >99%, with other trace metals. The TCE (99.5+%, GR grade) was obtained from the Merck Company. Pentane (99.5+%, GR grade), also purchased from Riedel-deHaën, was used as the extractant. Sulfuric acid (97%), purchased from the Osaka Co. (Japan), was used to pretreat the iron. A standard chloride ion solution, obtained from Merck, was used to identify the qualities and quantities of chloride ion, as measured by an ion chromatograph (IC). The ammonium acetate ($C_2H_7NO_2$, Riedel-deHaën), acetic acid ($C_2H_6O_2$, Merck), 1,10-phenanthroline (Riedel-deHaën), ferrous chloride tetrahydrate ($FeCl_2{\cdot}6H_2O$, Fluke) and ferrous ammonium sulfate ($Fe(NH_4)_2(SO_4)_2{\cdot}6H_2O$, Ferak) were all GR grade. The DI water had a resistivity of 18.0 MΩ. The water was obtained from a Millipore-Q system. The Millipore-Q water was sparged with nitrogen gas for half an hour to ensure that the DO concentration remained below 0.5 mg/l, and thus emulated the low oxygen levels that are typical of actual groundwater.

### 2.2. Acid pretreatment of the iron

Acid-washed iron was used in some of the experiments. A 2.0 l beaker containing a known mass of powdered iron (that was measured prior to pretreatment) in 1.5 l of 1N sulfuric acid solution was agitated at 300 rpm for 0.5 h, then rinsed five times in 1.5 l deionized water to prevent any $H_2SO_4$ from remaining on the iron surface. Following the rinsing, the iron was dried for 2 days in a freeze-drying system (Labconco Co.) and then sieved using a 120 mesh screen (opening size of 0.125 mm). To inhibit oxidation, the iron powder was stored in nitrogen-sparged glass jars prior to use.

### 2.3. Dechlorination experiments

Each batch of experiments was conducted using 7.5 g of iron powder in 30 ml serum bottles that were filled with the deoxygenated solution. These deoxygenated solutions were prepared by purging, with $N_2$ (99.995%) at a flow rate of 5 l/min, to remove any trace amounts of oxygen left in the solution [20]. A 90 mg/l of TCE solutions were prepared by injecting appropriate quantities of pure TCE reagent into deoxygenated solutions, which were in the 1 l serum bottles without any headspace. The solutions were then immediately sealed and stirred to dissolve the TCE thoroughly. The ferrous ion solutions were prepared by dissolving $FeCl_2{\cdot}6H_2O$ as the ferrous source. Solutions containing both $Fe^{2+}$ and TCE were prepared, by adding a known mass of $FeCl_2{\cdot}6H_2O$ powder into deoxygenated solutions, after which TCE was injected and then proceeded the same as for the preparation of the TCE solutions. The ferrous iron concentrations in this study were 50, 100, and 300 mg/l.

To begin each batch of experiments, solutions were transferred into serum bottles containing acid-washed or unwashed iron, depending on the experimental requirements, and sealed immediately with Teflon-lined rubber septa. All the bottles were shaken in an orbital shaker at 30 rpm and room temperature (25–30 °C). In addition, control batches, without the addition of iron or ferrous ions, were also conducted. The experimental process lasted for 72 h. The TCE concentrations in the test bottles were measured at intervals time. Fifty microliters aliquots of solution were withdrawn using a 250 μl gastight syringe.

After withdrawing from the solutions, the bottle caps were removed and the pH and redox potential (SUNTEX, SP-701) of the solutions in the bottles immediately were measured. The solutions were then filtered through a membrane filter with a pore diameter of 0.45 μm (ADRANTEC MFS, Inc.). The filtered solutions were collected and the total dissolved iron, ferrous and chloride ion concentrations were determined. Residual particles on the membrane were freeze-dried and prepared for SEM-EDS and XPS observation.

### 2.4. Analytical methods

#### 2.4.1. TCE concentration

TCE was extracted via a liquid–liquid extraction process using pentane. The aqueous samples were then transferred into 1.8 ml vials containing 1.0 ml of pentane. The extraction vials

were placed on an orbital shaker and shaken at 150 rpm for 2 h. Following extraction, 1 μl of the sample was withdrawn from the pentane layer and injected into a gas chromatograph (GC), which was operated in splitless mode. The TCE concentrations were measured using a GC (HP-6890) equipped with an electron capture detector (ECD) and a DB-624 capillary column (30 m × 0.53 mm in size; 3 μm film in thickness; made by J & W). The flow rate of the carrier gas (99.999% $N_2$) was 6 ml/min. The temperatures of the oven, the inlet and the detector were maintained at 100, 200 and 250 °C, respectively.

#### 2.4.2. Concentration of inorganic ions

The concentration of dissolved chloride ions in the solution was measured at the end of each batch of experiments using an ion chromatograph (Dionex Model 4500i). The pH values were kept lower than 2 by adding drops sulfuric acid to the filtered solutions in order to prevent the iron from precipitating as ferrous hydroxide. The total concentration of dissolved iron was determined by atomic absorption spectrometry (Varian, 400). The concentration of ferrous ions was determined by the phenanthroline method [21] with a spectrophotometer (GBC, UV-911).

#### 2.4.3. SEM and EDS

Scanning electron micrographs (SEM) were generated using a Hitachi S-800 field emission secondary electron microscope and a Kevex Level III EDS analyzer, to observe the deposition phenomena on the iron surface. Images were collected at a beam potential of 20 kV. The precipitates on the iron surface were analyzed using EDS to determine the elements present.

#### 2.4.4. XPS

XPS was performed using a VG-Scientific Sigma Probe X-ray photoelectron spectrometer, with a monochromatized Al Kα X-ray source, operated at a power of 108 W. The samples were pressed into flat wafers and mounted on a sample holder. All the samples were stored in a nitrogen atmosphere to prevent atmospheric contamination and oxidation. Survey scans in the binding energy range from 0 to 800 eV were used to identify all detectable elements on the samples: C, Fe, O, Si and Ca. Quantification of the atomic composition of Fe was carried out. The peaks were integrated with the aid of the Shirley background subtraction algorithm, and then these peak areas converted to compounds percentages via the sensitivity factors included in the Avantage system software [22,23].

## 3. Results and discussion

### 3.1. Dependence of TCE degradation on iron pretreatment

#### 3.1.1. TCE degradation

The experimental results in Fig. 1 indicate that the reductive dechlorination of TCE occurred when acid-washed iron was used. TCE was absent from the system after the reactions had proceeded for 37 h. Previous studies [24–26] have shown that the degradation rate of TCE by ZVI, with respect to the contaminant concentration, can be described by a pseudo-first-order kinetic

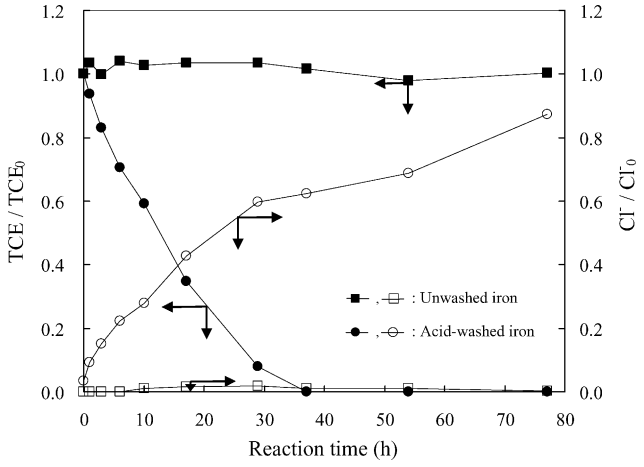


Fig. 1. Effect of the pretreatment of zero-valent iron on TCE dechlorination.

model, where the rate is proportional to the TCE concentration ([TCE]):

$$\frac{\mathrm{d[TCE]}}{\mathrm{d}t} = -k_{\mathrm{obs}}[\mathrm{TCE}] \quad (1)$$

and where $k_{\mathrm{obs}}$ ($\mathrm{h}^{-1}$) is the observed first-order rate constant. The integration of Eq. (1) results in

$$[\mathrm{TEC}] = [\mathrm{TEC}]_0\, \mathrm{e}^{-k_{\mathrm{obs}}t} \quad (2)$$

where $[\mathrm{TCE}]_0$ is the initial TCE concentration and $t$ is reaction time. The observed first-order rate constants can be calculated from the regression of ln([TCE]) versus time. The observed rate constant calculated herein was 0.084 $\mathrm{h}^{-1}$, as shown in Table 1. In addition, the percentage of chloride released was accompanied by an increase in amount of TCE removed, which proves that the reductive dechlorination of TCE had occurred. However, the percentage of chloride released at the end of the reaction was found to be only 88% less than the theoretical value. This difference could have been caused by the formation of end or intermediate chlorinated products, which were ineffectively dechlorinated during the limited reaction time [26,27]. Fig. 2 also shows that the ORP dropped rapidly, from an initial value of 252 to −485 mV, indicating the reductive conditions that were proved in aqueous solution. Conversely, as seen in Fig. 1, TCE degradation did not occur when the ZVI was unwashed. Both the concentration of chloride and the potential varied, indicating that the pretreatment of ZVI by acid-washing had a significant effect on the reductive dechlorination of TCE [26,28–30].

Table 1
The observed pseudo-first-order rate constants, $k_{\mathrm{obs}}$, for TCE degradation under the different experimental conditions

| Addition of $Fe^{2+}$ (mg/l) | $k_{\mathrm{obs}}$ ($\mathrm{h}^{-1}$) | |
|---|---|---|
| | Acid-washed iron | Unwashed iron[a] |
| 0 | 0.084 | 0 |
| 50 | 0.066 | 0.011 |
| 100 | 0.054 | 0.018 |
| 300 | 0.044 | 0.023 |

[a] Rate constants calculated as the TCE degradation occurred.

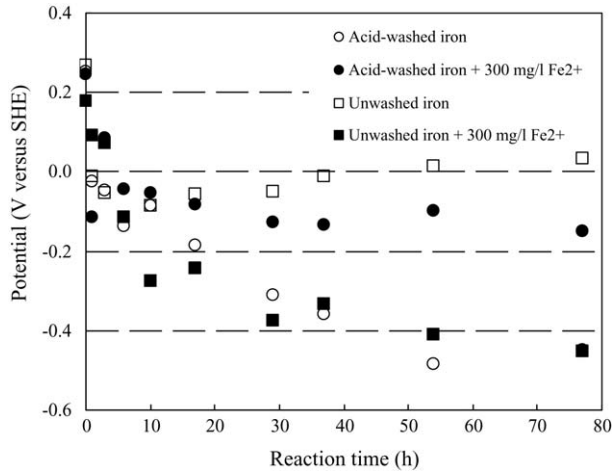


Fig. 2. Potential vs. time, as measured by the degradation of TCE.

### 3.1.2. Observation of the iron surface

Fig. 3(a) indicates that unwashed iron exhibited a mixture of impurities, including elements Si and Ca, as revealed by the overall X-ray photoelectron spectrum of the iron surface. The impurity on iron metal inhibited iron surface corrosion and TCE reduction [28]. Fig. 3(a) also reveals that acid-washing of iron could decrease the impurity content. Consequently, an X-ray photoelectron spectrum of a "clean" iron surface was obtained.

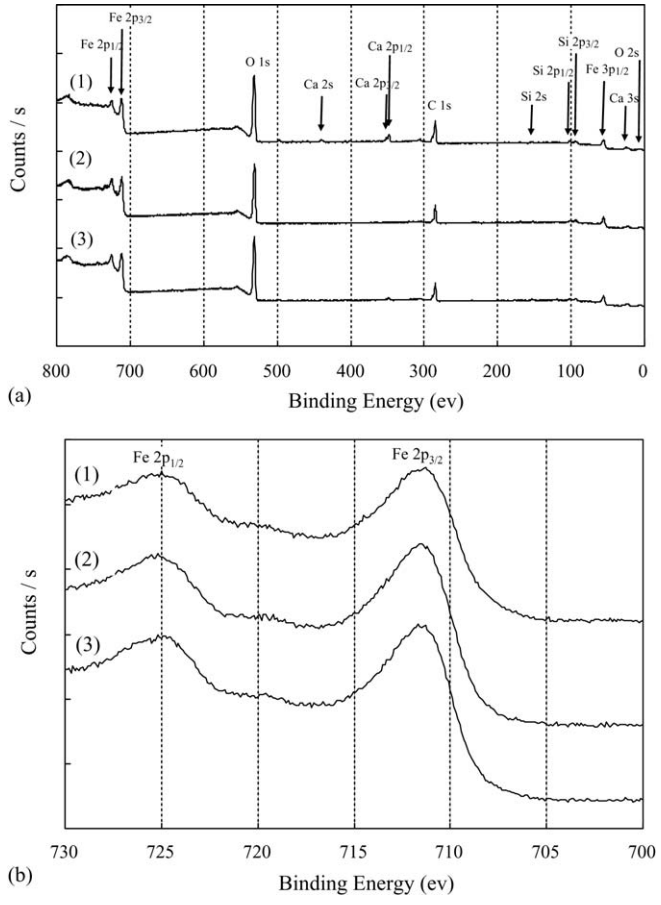


Fig. 3. (a) Full-scan (b) Fe 2p photoelectron spectrum of the iron surface ((1) before, (2) after pretreatment by acid-washing, and (3) exposure to an aqueous solution of TCE after iron pretreatment).

Fig. 3(b) shows the Fe 2p XPS region of the iron surface before and after acid-washing. The Fe $2p_{3/2}$ peak at 712.4 eV is indicative of ferric iron, which could be present in any one of several possible forms. The curves were fitted by the peaks of the various possible iron oxide and oxyhydroxide species. Then, the composition and content of iron (hydro) oxides were calculated using a database and computer software analysis. The results in Table 2 indicate that hydrated ferric oxide, such as goethite (α-FeOOH, 85%) and maghemite (γ-$Fe_2O_3$, 12%) on the iron surface before acid-washing. Free energy thermodynamic considerations require that goethite is hydrolyzed into various hydroxyl species in the solution. Also, the reduction conditions enhance the solubility of goethite by promoting reductive dissolution ($\alpha\text{-FeOOH} + e^- + 3H^+ \rightarrow Fe^{2+} + 2H_2O$) [10]. It is suggested that the passive layer on the iron surface is maghemite [31]. Ritter et al. [32] found that an impure commercial material would be converted into a passive layer of maghemite by the high-temperature oxidation procedure used in the production of iron. Understanding the behavior of this layer when it comes into contact with a solution is important, because maghemite inhibits electron transfer and catalytic hydrogenation. This means that TCE removal from raw iron that has not been acid-washed is ineffective.

On the other hand, Table 2 indicates that α-FeOOH (95%), $Fe_2O_3$ (1.8%) and $Fe_3O_4$ (3%) of iron oxyhydroxides formed on the surface of acid-washed iron, revealing that acid-washing reduced the $Fe_2O_3$ content in the passive layer, whereas the $Fe_3O_4$ content was increased. Although $Fe_3O_4$ is also proposed to form one of the passive layers, its semiconductive properties are such that electron transport from the underlying ZVI to the solid/liquid interface can occur. Thus, the acid-washing pretreatment of ZVI can increase the number of reactive sites, consequently enhancing the TCE degradation. In addition, XPS measurements revealed that the characteristics of the iron surface after 77 h of TCE treatment were the same as those of the initial acid-washed iron, indicating that the surface of the iron remained reactive. Although the overall surface composition changed only slightly, acid-washing altered the relative abundance of the specific iron oxyhydroxides species. Thus, the pretreatment of the iron clearly affected both the relative surface abundance and the bonding of each element.

## 3.2. TCE degradation using ZVI in the presence of ferrous irons

### 3.2.1. Acid-washed iron

Fig. 4(a) shows that, when acid-washed iron was used, the rate of TCE degradation and the percentage of chloride released decreased as the concentration of ferrous ions increased. When the ferrous concentration increased from 0 to 300 mg/l, Table 1 shows that the observed pseudo-first-order rate constant of the TCE degradation declined from 0.084 to 0.044 $h^{-1}$. Moreover, the percentage of chloride released did not reach 100% even though the TCE had been completely removed by the end of the reaction. The percentage of unreleased chloride in the system

Table 2
Composition and content of iron (hydro) oxides on an iron surface in various conditions as determined by XPS analysis

| Composition | Acid-washed iron | Unwashed iron | After addition of $Fe^{2+}$ with | |
|---|---|---|---|---|
| | | | Acid-washed iron[a] | Unwashed iron[a] |
| α-FeOOH (%) (goethite) | 95 | 85 | 71 | 81 |
| γ-$Fe_2O_3$ (%) (maghemite) | 1.8 | 12 | 27 | 3 |
| $Fe_3O_4$ (%) (magnetite) | 3 | –[b] | 2 | 12 |

[a] Reaction with TCE for $Fe^{2+}$: 300 mg/l and TCE: 90 mg/l, respectively.
[b] Not detectable.

was greater than that associated with TCE degradation using only ZVI, because the extra added ferrous ions seemed to interfere with the TCE degradation. Fig. 2 reveals that the potential dropped rapidly in the initial 18 h of the reaction, but after this time no further change occurred. The variation in the rate constants for TCE degradation, given these potential conditions, reveals that some reductive dechlorination reactions of TCE by acid-washed iron will be affected when extra ferrous ions are added.

When ZVI was used to treat the TCE, without the addition of ferrous ions, the measurements of pH show that the initial pH of 7 increased to 9. Ritter et al. [32] has stated that under anaerobic conditions iron can be oxidized by the introductions of chloroorganics (Eq. (3)) or water (Eq. (4)) so the pH value increases, as follows:

$$Fe^0 + RCl + H^+ \rightarrow Fe^{2+} + RH + Cl^- \quad (3)$$

$$Fe^0 + 2H_2O \rightarrow Fe^{2+} + H_{2(g)} + 2OH^- \quad (4)$$

However, the consequent rise in pH can cause the precipitation of ferrous hydroxide:

$$Fe^{2+} + 2OH^- \rightarrow Fe(OH)_{2(s)} \quad (5)$$

On the other hand, an examination of Fig. 4(b) shows that the concentration of ferrous ions decreased after the reactions had proceeded for 3 h with the addition of ferrous ions. Furthermore, the greater the amount of ferrous ions that were added, accompanied by the consumption of hydroxyl ions, the larger the amount of ferrous hydroxide precipitates, as shown in Eq. (5). Thus, the pH value decreased to a neutral level. Ferrous hydroxide is thermodynamically unstable and may be further oxidized to form magnetite (see Eq. (6)), when the pH is higher than 6–7 [8]:

$$Fe(OH)_{2(s)} \rightarrow Fe_3O_{4(s)} + H_{2(g)} + 2H_2O \quad (6)$$

It is proposed that there is a passive layer of magnetite that can interfere with the degradation of the contaminants. However, as the precipitates age, the electron-conducting magnetite is oxidized to form maghemite with a near neutral pH, which stops electron transfer from the $Fe^0$ core and halts the redox reaction.

The SEM observations of the iron surface, displayed in Fig. 5, demonstrate that, by the end of reaction, several precipitates had formed coating the iron surface, which verifies the above statement. Also, the formation of precipitates on the iron surface clearly increased with the ferrous ion concentration, indicating that TCE degradation by ZVI was seriously inhibited. Table 2 indicates that in the reactions of TCE degradation using ZVI, the maghemite content increased from 1.8 to 27%. In addition, the residual particles collected from the bulk solution after the reaction, which were quantified by SEM-EDS analysis, had an iron to oxygen elemental molar ratio of 3:3.94, which is near that of magnetite. The precipitates in the bulk solution were indeed magnetite, meaning that Eq. (6) can be applied. Consequently, both maghemite and magnetite could be found after the TCE was degraded by ZVI in the presence of ferrous ions. These compounds inhibited electron transfer and catalytic hydrogenation, causing the rate of TCE degradation declined.

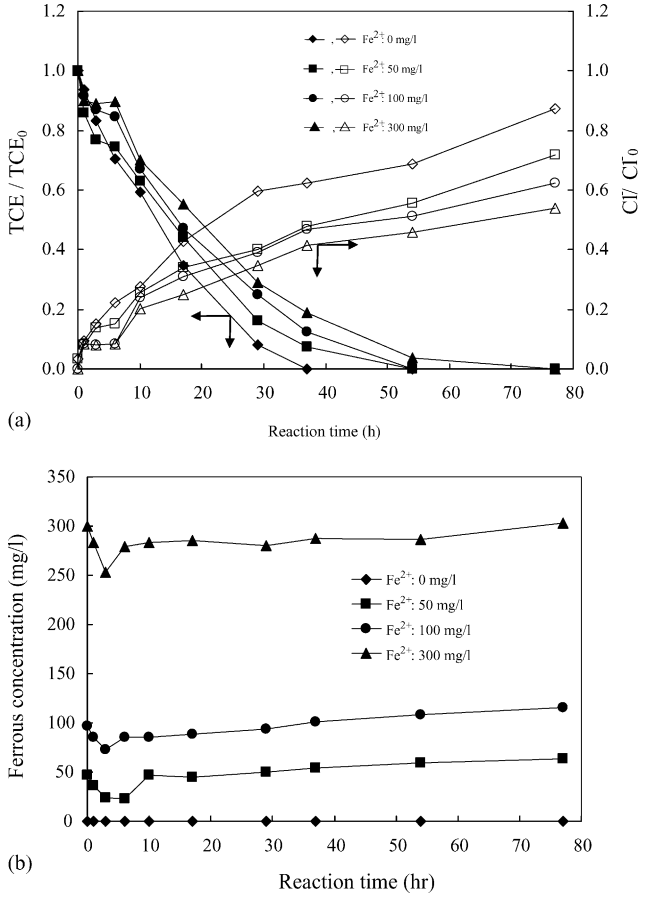


Fig. 4. (a) Relative concentrations of TCE and $Cl^-$, and (b) ferrous ion concentrations for TCE dechlorination in the presence of acid-washed metallic iron, with various ferrous ion concentrations.

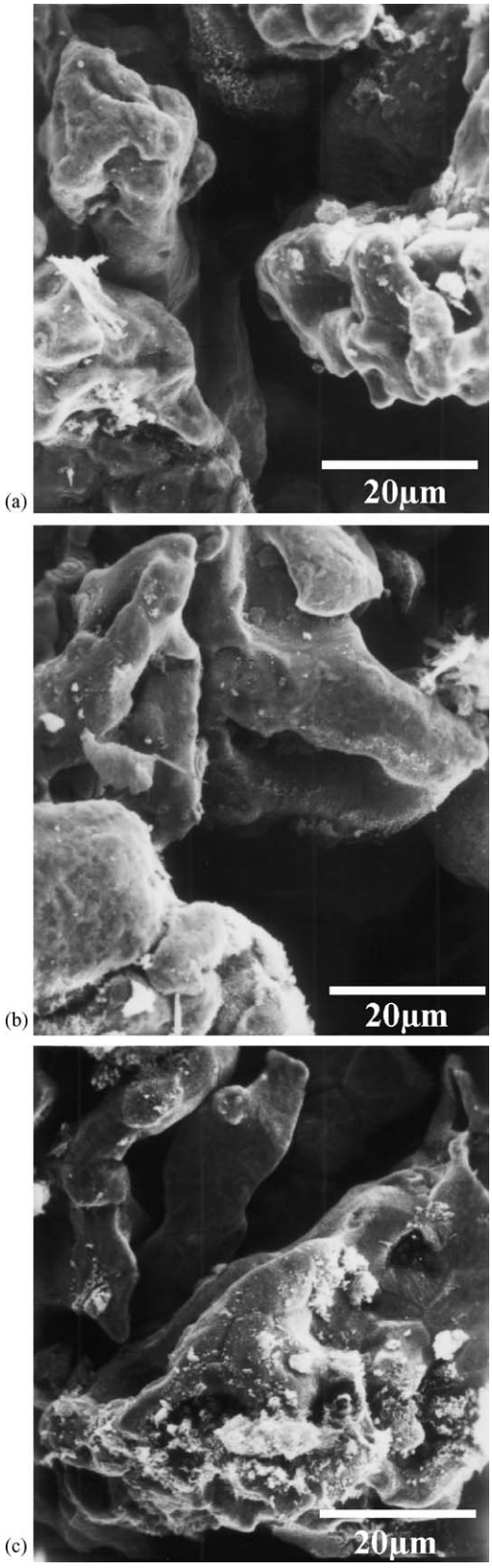


Fig. 5. Scanning electron micrograph (SEM) of the iron surface for TCE dechlorination after the acid-washing pretreatment of zero-valent iron, with various ferrous ion concentrations: (a) $Fe^{2+}$, 50 mg/l; (b) $Fe^{2+}$, 100 mg/l; (c) $Fe^{2+}$, 300 mg/l.

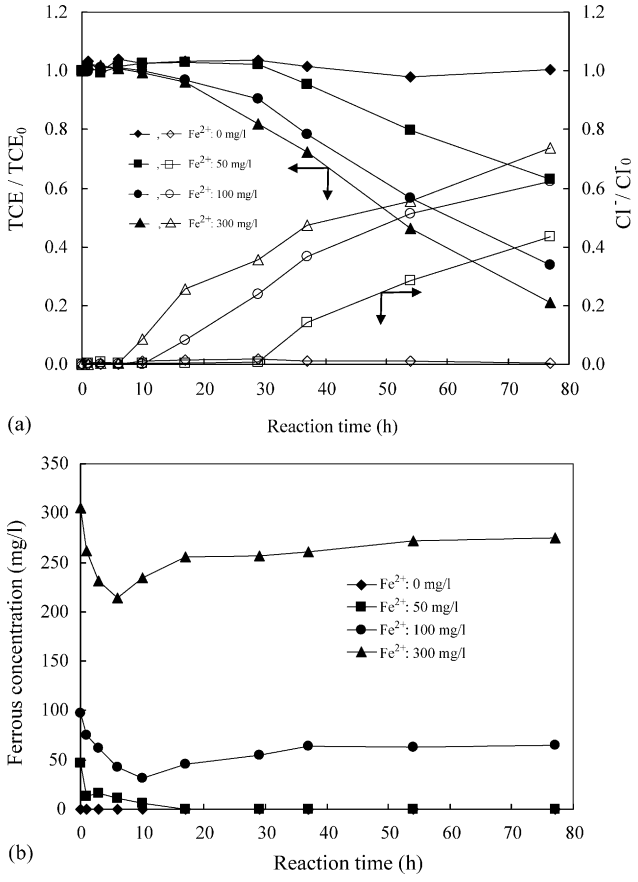


Fig. 6. (a) Relative concentrations of TCE and $Cl^-$, and (b) ferrous ion concentrations for TCE dechlorination in the presence of unwashed metallic iron, with various ferrous concentrations.

### 3.2.2. *Unwashed iron*

Fig. 6(a) clearly shows that when the iron was unwashed and the initial concentration of ferrous ion was 50 mg/l, the TCE concentration decreased after 29 h of reaction time. Furthermore, the TCE concentration also dropped significantly when the initial concentration of added ferrous ions increased to 300 mg/l. Table 1 also reveals the increase of TCE degradation rate constant with the increase of ferrous ion. However, all the TCE could not be completely removed by the end of reaction time. This enhanced TCE degradation indicated that some surface reactions on the unwashed iron still proceeded in the presence of ferrous ions.

Fig. 6(b) shows that the measured ferrous concentration decreased during the initial 10 h of reaction time, thus indicating that some ferrous ions were adsorbed and incorporated into the iron surface. In Table 2, XPS analysis shows that treatment with TCE increased the magnetite content on the iron surface to 12% when 300 mg/l of ferrous ions were added.

Farrell et al. [33] has proposed the following two-layer semiconductor model. The passive layer on ZVI consists of an inner layer, a semiconductor with good (metallic) conductivity (such as magnetite) and an outer layer, a semiconductor with poorer conductivity than the metallic conductivity (such as maghemite). Although magnetite is a semiconductor, the small band gap between its valence and the conduction bands gives it an electri-

cal conductivity close to that of metal. Therefore, magnetite is not considered to be a passivation oxide. In contrast to magnetite, maghemite has a large band gap and is regarded as a passivation oxide [10,33]. However, the adsorption and incorporation of aqueous ferrous ions into the maghemite lattice, where the maghemite is locally converted to magnetite, enhances the conductivity of the oxide layer and allows electrons to be transferred from $Fe^0$ to the contaminant at the oxide–water interface [18].

The above results and interpretations indicate that ferrous ions were adsorbed on the iron surface, converting the precipitates to magnetite form, consequently, the reductive dechlorination of TCE continues. However, the low resistance caused by the high conductivity of the magnetite layer does not allow electrons to migrate freely from inside to outside. Therefore, the TCE degradation proceeds more slowly since the charge transfer rate through an oxide is lower than on acid-washed ZVI surface when extra ferrous ions are added in the presence of ZVI.

## 4. Conclusions

The TCE reactions with ZVI have been shown to depend on the condition of the surface of the iron. Unwashed iron, with the ineffective TCE degradation, exhibited a mixture of impurities, such as elemental Si and Ca. Also, the predominant species on the iron surface, as determined by XPS analysis were goethite (α-FeOOH) 85% and maghemite (γ-$Fe_2O_3$) 12%. Goethite undergoes hydrolysis and dissolution into its various hydroxyl species. Maghemite formed a passive layer on the surface of the iron, which inhibited electron transfer and catalytic hydrogenation. However, acid-washed iron, with its higher first-order rate constant for TCE degradation, had a changed composition and iron oxyhydroxide content on the surface of iron. Acid-washing reduced the maghemite content in the passive layer, meanwhile the magnetite content was insignificantly increased. Magnetite owned the semiconductive properties, such as electron transport from the underlying ZVI to the solid/liquid interface. Therefore, the increase in the number of reactive sites, the higher electron transfer velocity, and the repeatable initial surface conditions, all promoted the oxidation of the acid-washed iron, and thus enhanced the TCE degradation.

However, in water, when ferrous ions were simultaneous with TCE, the TCE degradation rate decreased as the ferrous ion concentration increased. The precipitation of ferrous hydroxide from both the magnetite and maghemite that coated the surfaces of the acid-washed ZVI, consequently, inhibiting the electron transfer and catalytic hydrogenation mechanisms. Ferrous ions in the $Fe^0$-TCE system without acid-washing were adsorbed into a maghemite lattices; maghemite was converted into semiconductive magnetite material. Thus, these electrons passed through the precipitates on the iron surface, enabling the reductive dechlorination of TCE. However, the TCE degradation would proceed more slowly, since the change transfer rate through an oxide is slower than on acid-washed ZVI surface, when extra ferrous ions are added.

The results suggest that TCE degradation rate constant decreased with the increase of the ferrous ion using acid-washed ZVI. Conversely, the increase of the ferrous ion significantly promoted TCE degradation using unwashed ZVI. This behavior explained that why the untreated iron using in PRBs is effective with ferrous ion incorporation. However, the intermediate or end products, with respect to TCE degradation by alternative ZVI at different times, are not well understood. Further research is needed to better characterize the phenomena.

## Acknowledgement

The authors would like to thank the National Science Council of the Republic of China for financially supporting this research under Contract no. NSC 91-2211-E-008-025.

## References

[1] R.W. Puls, D.W. Blowes, R.W. Gillham, Long-term performance monitoring for a permeable reactive barrier at the U.S. Coast Guard Support Center, Elizabeth City, North Carolina, J. Hazard. Mater. 68 (1999) 109–124.
[2] A.R. Gavaskar, Design and construction techniques for permeable reactive barriers, J. Hazard. Mater. 68 (1999) 41–71.
[3] M.M. Scherer, S. Richter, R.L. Valentine, P.J.J. Alvarez, Chemistry and microbiology of permeable reactive barriers for in situ groundwater clean up, Crit. Rev. Env. Sci. Tec. 30 (2000) 364–411.
[4] United States Environmental Protection Agency, Permeable Reactive Subsurface Barrier for the Interception and Remediation of Chlorinated Hydrocarbon and Chromium(VI) Plumes in Ground Water, Nation Risk Management Research Laboratory Ada, OK74820, EPA/600/F-97/008, 1997.
[5] United States Environmental Protection Agency, Field Applications of in situ Remediation Technologies: Permeable Reactive Barriers, Office of Solid Waste and Emergency Response and Technology Innovation Office, Washington, DC 20460, 2002.
[6] A. Agrawal, W.J. Ferguson, B.O. Gardner, J.A. Christ, J.Z. Bandstra, P.G. Tratnyek, Effects of carbonate species on the kinetics of dechlorination of 1,1,1-trichloroethane by zero-valent iron, Environ. Sci. Technol. 36 (2002) 4326–4333.
[7] R. Köber, O. Schlicker, M. Ebert, A. Dahmke, Degradation of chlorinated ethylenes by $Fe^0$: inhibition processes and mineral precipitation, Environ. Geol. 41 (2002) 644–652.
[8] P.D. Mackenzie, D.P. Horney, T.M. Sivavec, Mineral precipitation and porosity losses in granular iron column, J. Hazard. Mater. 68 (1999) 1–17.
[9] S. Yabusaki, K. Cantrell, B. Sass, C. Steefel, Multicomponent reactive transport in an in situ zero-valent iron cell, Environ. Sci. Technol. 35 (2001) 1493–1503.
[10] R.M. Cornell, U. Schwertmann, The Iron Oxides, VCH Publishers, New York, 1996.
[11] M.S. Odziemkowski, T.T. Schuhmacher, R.W. Gillham, E.J. Reardon, Mechanism of oxide film formation on iron in simulating groundwater solutions: Raman spectroscopic studies, Corros. Sci. 40 (1998) 371–389.
[12] P.M.L. Bonin, M.S. Odziemkowski, R.W. Gillham, Influence of chlorinated solvents on polarization and corrosion behaviour of iron in borate buffer, Corros. Sci. 40 (1998) 1391–1409.
[13] P.M.L. Bonin, W. Jędral, M.S. Odziemkowski, R.W. Gillham, Electrochemical and Raman spectroscopic studies of the influence of chlorinated solvents on the corrosion behaviour of iron in borate buffer and in simulated groundwater, Corros. Sci. 42 (2000) 1921–1939.
[14] T.L. Johnson, W. Fish, Y.A. Gorby, P.G. Tratnyek, Degradation of carbon tetrachloride by iron metal: complexation effects on the oxide surface, J. Contam. Hydrol. 29 (1998) 379–398.
[15] A.G.B. Williams, M.M. Scherer, Spectroscopic evidence for Fe(II)–F(III) electron transfer at the iron oxide–water interface, Environ. Sci. Technol. 38 (2004) 4782–4790.

[16] J. Klausen, S.P. Tröber, S.B. Haderlein, R.P. Schwarzenbach, Reduction of substituted nitrobenzenes by Fe(II) in aqueous mineral suspensions, Environ. Sci. Technol. 29 (1995) 2396–2404.
[17] L. Charlet, E. Liger, P. Gerasimo, Decontamination of TCE- and U-rich water by granular iron: role of sorbed Fe(II), J. Environ. Eng. ASCE 124 (1998) 25–30.
[18] Y.-H. Huang, T.-C. Zhang, Kinetics of nitrate reduction by iron at near neutral pH, J. Environ. Eng. ASCE 128 (2002) 604–611.
[19] T.B. Hofstetter, R.P. Schwarzenbach, S.B. Haderlein, Reactivity of Fe(II) species associated with clay minerals, Environ. Sci. Technol. 37 (2003) 519–528.
[20] R.A. Maithreepala, R.-A. Doong, Reductive dechlorination of carbon tetrachloride in aqueous solutions containing ferrous and copper ions, Environ. Sci. Technol. 38 (2004) 6676–6684.
[21] A.D. Eaton, L.S. Clesceri, A.E. Greenberg, Standard Methods for the Examination of Water and Wastewater, 19th ed., APHA, Washington, 1995.
[22] J.F. Watts, An Introduction to Surface Analysis by Electron Spectroscopy, Oxford University Press, Royal Microscopical Society, New York, 1990.
[23] J.F. Moulder, W.F. Stickle, O.E. Sobol, K.D. Bomben, Handbook of X-ray Photoelectron Spectroscopy, Physical Electronics, Inc., Minnesota, 1995.
[24] L.J. Matheson, P.G. Tratnyek, Reductive dehalogenation of chlorinated methanes by iron metal, Environ. Sci. Tecnol. 28 (1994) 2045–2053.
[25] B.R. Helland, P.J.J. Alvarez, J.L. Schnoor, Reductive dechlorination of carbon tetrachloride with elemental iron, J. Hazard. Mater. 41 (1995) 205–216.
[26] C. Su, R.W. Puls, Kinetics of trichloroethene reduction by zero-valent iron and tin: pretreatment effect, apparent activation energy, and intermediate products, Environ. Sci. Tecnol. 33 (1999) 163–168.
[27] W.S. Orth, R.W. Gillham, Dechlorination of trichloroethene in aqueous solution using $Fe^0$, Environ. Sci. Technol. 30 (1996) 66–71.
[28] M.L. Támara, E.C. Butler, Effects of iron purity and groundwater characteristics on rates and products in the degradation of carbon tetrachloride by iron metal, Environ. Sci. Technol. 38 (2004) 1866–1876.
[29] N. Ruiz, S. Seal, D. Reinhart, Surface chemical reactivity in selected zero-valent iron samples used in groundwater remediation, J. Hazard. Mater. 80 (2000) 107–117.
[30] C.L. Geiger, N.E. Ruiz, C.A. Clausen, D.R. Reinhart, J.W. Quinn, Ultrasound pretreatment of elemental iron: kinetic studies of dehalogenation reaction enhancement and surface effects, Water Res. 36 (2002) 1342–1350.
[31] W. Stumm, Chemistry of the Solid–Water Interface, John Wiley & Sons, Inc., New York, 1992.
[32] K. Ritter, M.S. Odziemkowski, R.W. Gillham, An in situ study of the role of surface films on granular iron in the permeable iron wall technology, J. Contam. Hydrol. 55 (2002) 87–111.
[33] J. Farrell, M. Kason, N. Melitas, T. Li, Investigation of the long-term performance of zero-valent iron for reductive dechlorination of trichloroethylene, Environ. Sci. Technol. 34 (2000) 514–521.